

RESEARCH

Open Access



By activating endothelium histone H4 mediates oleic acid-induced acute respiratory distress syndrome

Yanlin Zhang^{1*}, Jingjin Tan¹, Yiran Zhao¹, Li Guan¹ and Shuqiang Li^{1*}

Abstract

Objective This study investigated pathogenic role and mechanism of extracellular histone H4 during oleic acid (OA)-induced acute respiratory distress syndrome (ARDS). Methods: ARDS was induced by intravenous injection of OA in mice, and evaluated by blood gas, pathological analysis, lung edema, and survival rate. Heparan sulfate (HS) degradation was evaluated using immunofluorescence and flow cytometry. The released von Willebrand factor (vWF) was measured using ELISA. P-selectin translocation and neutrophil infiltration were measured via immunohistochemical analysis. Changes in VE-cadherin were measured by western blot. Blocking antibodies against TLRs were used to investigate the signaling pathway. Results: Histone H4 in plasma and BALF increased significantly after OA injection. Histone H4 was closely correlated with the OA dose, which determined the ARDS severity. Pretreatment with histone H4 further aggravated pulmonary edema and death rate, while anti-H4 antibody exerted obvious protective effects. Histone H4 directly activated the endothelia. Endothelial activation was evidently manifested as HS degradation, release of vWF, P-selectin translocation, and VE-Cadherin reduction. The synergistic stimulus of activated endothelia was required for effective neutrophil activation by histone H4. Both TLRs and calcium mediated histone H4-induced endothelial activation. Conclusions: Histone H4 is a pro-inflammatory and pro-thrombotic molecule in OA-induced ARDS in mice.

Significance Statement

As the main risk factor for acute respiratory distress syndrome (ARDS), pulmonary fat embolism (PFE) is a common complication following long bone fractures, cardiopulmonary resuscitation, and infusion through an intraosseous catheter. This study showed that histone H4 is an essential pro-inflammatory and pro-thrombotic molecule in OA-induced ARDS. Histone H4 directly induces pulmonary endothelial activation. Endothelial activation is an indispensable synergistic stimulus for neutrophil activation induced by histone H4. TLRs and calcium are intimately involved in histone H4 mediated endothelium activation.

Keywords Acute respiratory distress syndrome, Pulmonary fat embolism, Oleic acid, Extracellular histone H4, Pulmonary endothelium

*Correspondence:

Yanlin Zhang
zhangyanlin@bjmu.edu.cn
Shuqiang Li
shuqiangli@263.net

¹Research Center of Occupational Medicine, Peking University Third Hospital, Beijing 100191, China



© The Author(s) 2024. **Open Access** This article is licensed under a Creative Commons Attribution-NonCommercial-NoDerivatives 4.0 International License, which permits any non-commercial use, sharing, distribution and reproduction in any medium or format, as long as you give appropriate credit to the original author(s) and the source, provide a link to the Creative Commons licence, and indicate if you modified the licensed material. You do not have permission under this licence to share adapted material derived from this article or parts of it. The images or other third party material in this article are included in the article's Creative Commons licence, unless indicated otherwise in a credit line to the material. If material is not included in the article's Creative Commons licence and your intended use is not permitted by statutory regulation or exceeds the permitted use, you will need to obtain permission directly from the copyright holder. To view a copy of this licence, visit <http://creativecommons.org/licenses/by-nc-nd/4.0/>.

Introduction

Acute respiratory distress syndrome (ARDS) has a mortality rate of more than 40%. The hallmark of ARDS is refractory hypoxemia resulting from acute pulmonary proteinaceous edema [1–3]. Unchecked overwhelming inflammation triggered by injurious mediators is intimately involved with endothelial injury [4, 5]. Increased endothelial permeability is viewed as the underlying pathological basis of ARDS [6, 7]. Endothelial cells are not only damaged by inflammatory injury but also the active participants of inflammatory response. Activated endothelial cells may further aggravate the inflammatory response, resulting in a vicious circle [8, 9].

As the main risk factor for fatal ARDS, pulmonary fat embolism (PFE) is a common complication following long bone fractures, cardiopulmonary resuscitation, and infusion through an intraosseous catheter [10, 11]. PFE has many similarities with oleic acid (OA)-induced acute lung injury, but the underlying mechanisms remain largely unknown [12, 13]. Damage-associated molecular patterns (DAMPs) are considered to be a major pathway of uncontrolled inflammation. DAMPs molecules include extracellular histones, mitochondrial DNA, formyl peptides, HMBG1, etc. The role of DAMPs molecules has not been thoroughly investigated in OA-induced acute lung injury [14, 15].

Extracellular histones have been increasingly recognized as key mediators in systemic inflammatory injuries [16, 17]. Freeman et al. have proven that extracellular histones can bind pulmonary capillary endothelium preferentially through a charge-dependent interaction [18]. Therefore the aim of this study was to investigate the pathogenic role and mechanism of extracellular histone H4 during OA-induced ARDS.

Materials and methods

Reagents

The reagents used in this study included: oleic acid (OA) and Histopaque (Sigma-Aldrich St. Louis, MO, USA); histone H4 (Millipore, Billerica, MA, USA); antibodies for P-selectin, sodium-potassium ATPase, CD31 (PECAM-1), and Ly6G (Abcam, Cambridge, MA, USA); an antibody for Cadherin-5 (BD Transduction Laboratories, CA, USA); an antibody for heparan sulfate (HS) (Bioss, Woburn, MA, USA); blocking antibodies against P-selectin, TLR4 (HTA125), TLR2 (TL2.1), and TLR1 (GD2.F4) (eBioscience, San Diego, CA, USA); a blocking antibody against TLR6 (TLR6.127) (Abcam, Cambridge, MA, USA); enzyme-linked immunosorbent assay (ELISA) kits for histone H4 and von Willebrand factor (vWF) (Cusabio Biotech, Wuhan, China); and 1,2-bis(2-aminophenoxy) ethane N, N,N',N'-tetraacetic acid acetoxyethyl ester (EGTA-AM) (MedChemExpress, Monmouth Junction, NJ, USA). Following the previously

described methods a blocking antibody against histone H4 (anti-H4) was purified in autoimmune mice [19].

Animal studies

Eight-week-old male C57BL/6 mice weighing 20–22 g were purchased from Peking University Animal Center (Beijing, China). All procedures followed in this study were reviewed and approved by the Peking University Animal Care and Use Committee (No. LA201783). The study was conducted in accordance with ARRIVE guidelines for experimental studies [20]. The mice were housed in an air-conditioned specific pathogen free facility at 25°C. Upon arrival, mice were allowed to acclimate for three days before the experiment. To minimize animal suffering, the mice were administered anesthesia before surgery and medication after surgery for pain relief, and were humanely sacrificed by injecting ketamine (100 mg/kg) and xylazine (6 mg/kg) followed by cervical dislocation as soon as the experimental procedures were completed. After administering anesthesia with 1.5% sodium pentobarbital, mice in the OA group were injected with OA via the lateral tail vein. To analyze the dose-response of OA, the dose of 100, 200, 300, or 450 $\mu\text{L}/\text{kg}$ suspended in 50 μL phosphate-buffered saline (PBS) were injected intravenously. The dose of 300 $\mu\text{L}/\text{kg}$ was injected intravenously to study acute lung injury while the dose of 450 $\mu\text{L}/\text{kg}$ was injected for the survival analysis. As an intervention, histone H4 (10 mg/kg) or anti-H4 antibody (20 mg/kg) was injected through the lateral tail vein 30 min prior to OA challenge according to the reference and the pre-experiment [21]. An equivalent volume of PBS was injected into control mice using similar methods. To ensure the ubiquitous distribution of OA, the total volume injected was split into three equal parts, which were injected sequentially while the mice were placed in supine, 30° right lateral, and 30° left lateral positions [22].

Blood gas analysis

After the mice were anesthetized, whole blood was collected by puncturing the abdominal aorta. To analyze arterial partial oxygen pressure (PaO_2), whole blood (0.25 mL) was examined using a gas analyzer (Ciba Corning, Etobicoke, ON, Canada). ARDS was diagnosed using PaO_2 analysis ($\text{PaO}_2/\text{FiO}_2 \leq 300$ mmHg).

Measurement of histone H4 in plasma and bronchoalveolar lavage fluid (BALF)

Plasma was separated from whole blood by centrifugation at 1,000 $\times g$ for 10 min at 4 °C. Because bronchoalveolar lavage can interfere with the analysis of lung wet/dry mass ratio, BALF was obtained from a different group of mice rather than from the group used for wet/dry ratio analysis. The BALF was obtained by flushing the

lungs with 1 mL PBS, and then centrifuged at 1,000×g for 10 min to collect the supernatant. Histone H4 in the plasma and supernatant was measured using ELISA.

Pathological and immunohistochemical analyses of pulmonary tissues

Lung samples obtained from the right upper lobes were fixed with 4% formalin for 48 h at 25 °C. After being embedded in paraffin, the fixed tissues were cut into 5- μ m-thick sections. The tissues were stained with hematoxylin and eosin (H&E). The pathologists who were blinded to the study design scored microscopic injury for H&E-stained sections. The degree of injury was judged by the reported criteria that was based upon the variables: interstitial edema, hemorrhage, necrosis, atelectasis and neutrophil infiltration [23]. To analyze immunohistochemically neutrophil specific marker Ly6G, the sections were blocked with 1% hydrogen peroxide in methanol for 25 min and with 1% BSA in 0.05% Tween-20 for 15 min. Then, the sections were incubated with the primary antibody for Ly6G (1:50) for 30 min, followed by incubation with a biotin-labeled goat anti-rabbit secondary antibody. Peroxidase substrate was used to develop the sections. For each pulmonary section, three microscopic visual fields were randomly selected.

Assessment of P-selectin in pulmonary vasculature

Immunohistochemical detection of P-selectin was conducted after lung sections were fixed in 4% paraformaldehyde for 90 min at 4 °C. Following a previously described protocol, a venule was defined as positively stained if it had a brown reaction product on more than 50% of the circumference of its endothelium. Ten venules were analyzed for each lung section, and 18 sections were examined for each group. The percentage of positively stained venules was calculated [24, 25].

Immunofluorescence analysis of pulmonary tissues

As soon as the cryosections (8 μ m) of pulmonary tissues were air-dried, they were fixed in 4% formalin for 30 min. The sections were permeabilized in blocking buffer (5% goat serum+0.5% BSA+1% Triton X-100) and incubated with a primary antibody for HS proteoglycan (1:50) for 2 h at room temperature. An FITC-labeled goat anti-rabbit IgG secondary antibody was used to visualize the HS proteoglycan, whereas DAPI (Vector, CA, USA) was used for nuclear staining. The fluorescence images were obtained using a confocal laser scanning microscope (Carl Zeiss LSM 710, Germany).

Western blotting

Protein concentration was measured using a Bio-Rad Protein Assay Kit. To analyze the vascular endothelial cadherin (VE-Cadherin) in mouse lung vascular

endothelial cells (MLVECs), the cytoplasm and membrane were separated using a Cell Fractionation Kit (Cell Signaling Technology, Danvers, MA, USA). Equal quantities of protein lysates (40 μ g) were mixed with the loading buffer and fractionated by sodium dodecyl sulphate-polyacrylamide gel electrophoresis. The separated proteins were transferred onto polyvinylidene difluoride membranes. The membranes were probed using an anti-Cadherin-5 primary antibody (1:2,000) and an anti-sodium-potassium ATPase antibody (1:100,000) overnight at 4 °C. The bands were visualized using a chemiluminescence system.

MLVEC isolation and characterization

MLVECs were prepared following a previously prescribed method. Pulmonary tissues were diced into 1 mm³ sections and cultured in 60-mm culture dishes. Adherent cells were further purified using a biotin-labeled rat anti-mouse CD31 antibody, and then cultured in endothelial growth medium-2 supplemented with 10% fetal-bovine-serum at 37 °C in 5% CO₂. The MLVECs were characterized by their cobblestone morphology and positive staining for factor VIII-related antigen (Sigma-Aldrich) [26]. Before the cells were treated with histone H4 or blocking antibodies against TLR1, TLR2, TLR4, TLR6, and P-selectin, they were incubated in serum-free medium for 12 h.

Measurement of P-selectin translocation

P-selectin translocation in MLVECs was assessed following the previously described cell surface ELISA [27]. The cells were treated with histone H4 in the presence or absence of specific blocking antibodies against TLRs. After being fixed with 1% paraformaldehyde for 20 min, the cells were incubated with blocking solution (5% BSA) for 15 min, and then incubated with an anti-P-selectin antibody (1:100) for 90 min. Peroxidase activity was quantified with a plate reader at 450 nm. The average level of cell surface P-selectin in the control group was considered as the baseline value.

Purification of neutrophils from mouse bone marrow

Isolation of mouse neutrophils from bone marrow was performed following the previously described protocol. In brief, the cells were flushed out of the marrow cavity using Hanks' salt solution, which contains 2 mM EDTA (without magnesium and calcium). Histopaque density gradient was used to separate the remaining cells after the erythrocytes were abandoned. Through centrifugation (2,000 rpm, 40 min), neutrophils were found to be mainly located at the interface of Histopaque 1077 and 1119. The cellular viability was evaluated using Trypan blue dye exclusion assay. Neutrophil purity was assessed using Wright-Giemsa staining [28].

Neutrophil adhesion assay

According to the described protocol, adhesion assay of neutrophils to endothelium was evaluated using a color digital camera attached with a binocular microscope (Olympus, Japan). Purified neutrophils were incubated with MLVECs in a culture well for 15 min. Three fields of view were randomly selected for every culture well, and the number of adhered neutrophils/mm² was recorded. The neutrophil adhesion results were presented as the ratio of the experiment group results to the control group results (100%) to eliminate the variations in neutrophil adhesion across groups [29]. The adhesion assay of neutrophils to the endothelial cells was performed under two conditions: (1) Neutrophils were challenged with the plasma collected from OA challenged mice (OA-plasma) and then exposed to MLVECs unchallenged with histone H4. (2) Neutrophils were challenged with OA-plasma and then exposed to MLVECs challenged with histone H4.

Statistical analyses

The results are shown as the mean ± SD. All data were analyzed using GraphPad Prism v8.3.0 (San Diego, CA, USA). One-way ANOVA was used to analyze the statistical differences among groups, and Tukey's multiple comparisons test was used to analyze the differences between groups. The log-rank (Mantel-Cox) test was applied to analyze animal survival time. The correlation test was used to analyze the relationship of OA injected and histone H4 in plasma or BALF. A *p*-value < 0.05 was considered statistically significant.

Results

Pathogenic role of histone H4 in OA induced ARDS in mice

After OA challenge, plasma histone H4 and BALF histone H4 were significantly higher than those in the control group, especially when the OA dose exceeded 300 μL/kg, as shown in Fig. 1A and B. Significant positive correlations were observed between the doses of OA (from 100 to 450 μL/kg) and histone H4 in plasma ($r=0.9706$, $p=0.006$) and BALF ($r=0.9612$, $p=0.0091$). Refractory hypoxemia is the hallmark of ARDS. OA challenge caused obvious hypoxemia in mice in a dose dependent manner, as shown in Fig. 1C. The PaO₂ decreased to 55.17 ± 15.52 mmHg ($p=0.0002$, compared to the control group) when the OA dose reached 300 μL/kg. The pathological changes of the lungs were clear, and included widespread thickened pulmonary interstitium, obvious infiltration of inflammatory cells, alveolar collapse, and diffuse hemorrhage, as shown in Fig. 1D. The pathological score reached to 4.83 ($p=0.0057$, compared to the control group). As shown in Fig. 1E, the lung wet/dry mass ratio was significantly increased after OA challenge compared to the control group ($p=0.0008$). Pretreatment

with histone H4 further worsened the pulmonary edema, while pretreatment with anti-H4 antibody significantly improved it. Remarkably, histone H4 infusion alone also caused severe pulmonary edema. Ten mice (10/14) died within 72 h after being challenged with a lethal dose of OA (450 μL/kg), as shown in Fig. 1F. When pretreated with intravenous histone H4, nearly all mice (13/14) died within 72 h after OA challenge ($p=0.0909$, compared to the mice only challenged with OA). In contrast, five mice (5/14) died when pretreated with the anti-H4 antibody ($p=0.0462$, compared to the mice only challenged with OA). There was a statistically significant difference ($p=0.0005$) in the survival rates between the mice pretreated with histone H4 and anti-H4 antibody.

Pulmonary endothelial activation mediated by histone H4

After OA challenge, pulmonary endothelial activation was increased compared to the control group. HS was significantly degraded 12 h after OA challenge, as shown in Fig. 2A. Pretreatment with histone H4 further promoted HS degradation, while the anti-H4 antibody significantly reduced the HS degradation. Similarly, histone H4 infusion caused significant HS degradation. As shown in Fig. 2B, OA challenge was associated with greater release of vWF compared to the control group ($p=0.0012$). VE-Cadherin status is an indicator of microvascular permeability. As shown in Fig. 2C, after OA challenge, the membrane VE-Cadherin was significantly decreased compared to the control group ($p=0.0478$). Pretreatment with histone H4 increased the loss of VE-Cadherin, whereas pretreatment with the anti-H4 antibody showed a protective effect. Pulmonary veins exhibited significant P-selectin translocation, as the proportion of veins that were positively stained for P-selectin was significantly increased compared to the control group ($p<0.0001$), as shown in Fig. 2D. Pretreatment with histone H4 and the anti-H4 antibody showed opposite effects on both vWF release and P-selectin translocation.

Neutrophil activation mediated by histone H4

Neutrophil infiltration and activation were increased in the lung tissues compared to the control group after OA challenge. As shown in Fig. 3A, staining for the specific neutrophil marker Ly6G showed that there was increased neutrophil infiltration into lung tissues. The MPO activity in the lung tissues was also significantly increased compared to the control group ($p<0.0001$), as shown in Fig. 3B. The serine proteases proteinase 3 and elastase were abundant in neutrophils and were released upon neutrophil degranulation. As shown in Fig. 3C and D, circulating proteinase 3 and elastase were significantly increased 12 h after OA challenge compared to the control group ($p<0.0001$). Pretreatment with histone H4 aggravated both neutrophil infiltration and activation

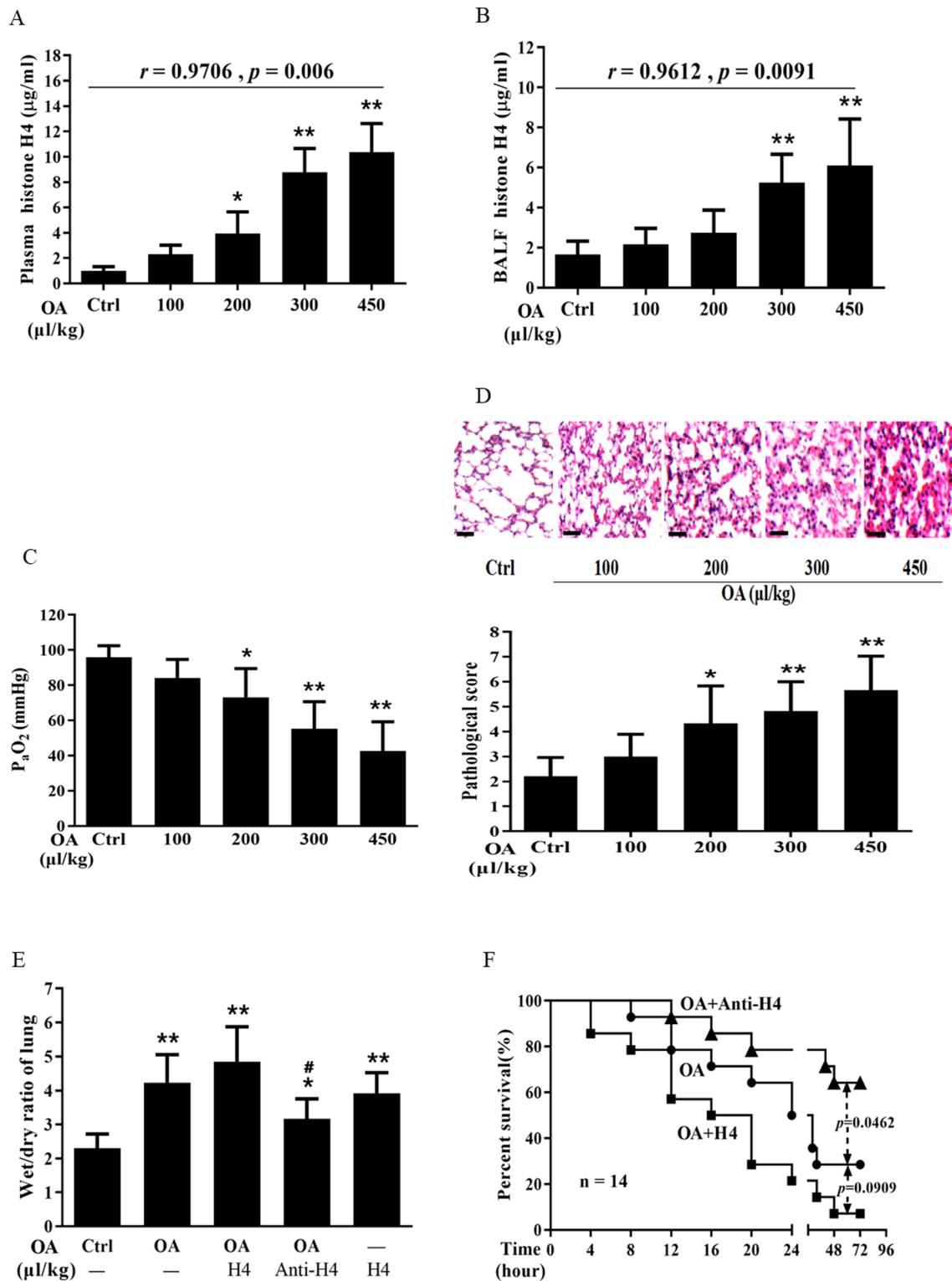


Fig. 1 Pathogenic role of histone H4 in OA-induced ARDS. Twelve hours after the mice were challenged with different intravenous doses of OA (100, 200, 300, or 450 $\mu\text{l/kg}$), histone H4 in the plasma (A), H4 in the BALF (B), blood gas (C), and pathological changes in lungs (D) were evaluated. Histone H4 (10 mg/kg) or anti-H4 antibody (20 mg/kg) was injected through the tail vein 30 min prior to OA challenge (300 $\mu\text{l/kg}$ for Figs. 1E and 450 $\mu\text{l/kg}$ for Fig. 1F). Then, the lung wet/dry mass ratio (E) and survival rate (F) were analyzed. Data are presented as mean \pm SD ($n = 14$ for the groups in Fig. 1F, and $n = 6$ for all other groups). The H&E stained lung sections are representative of three similar samples. Scale bars: 50 μm . * $p < 0.05$, ** $p < 0.01$ compared to the control group; # $p < 0.05$, ## $p < 0.01$ compared to the OA group

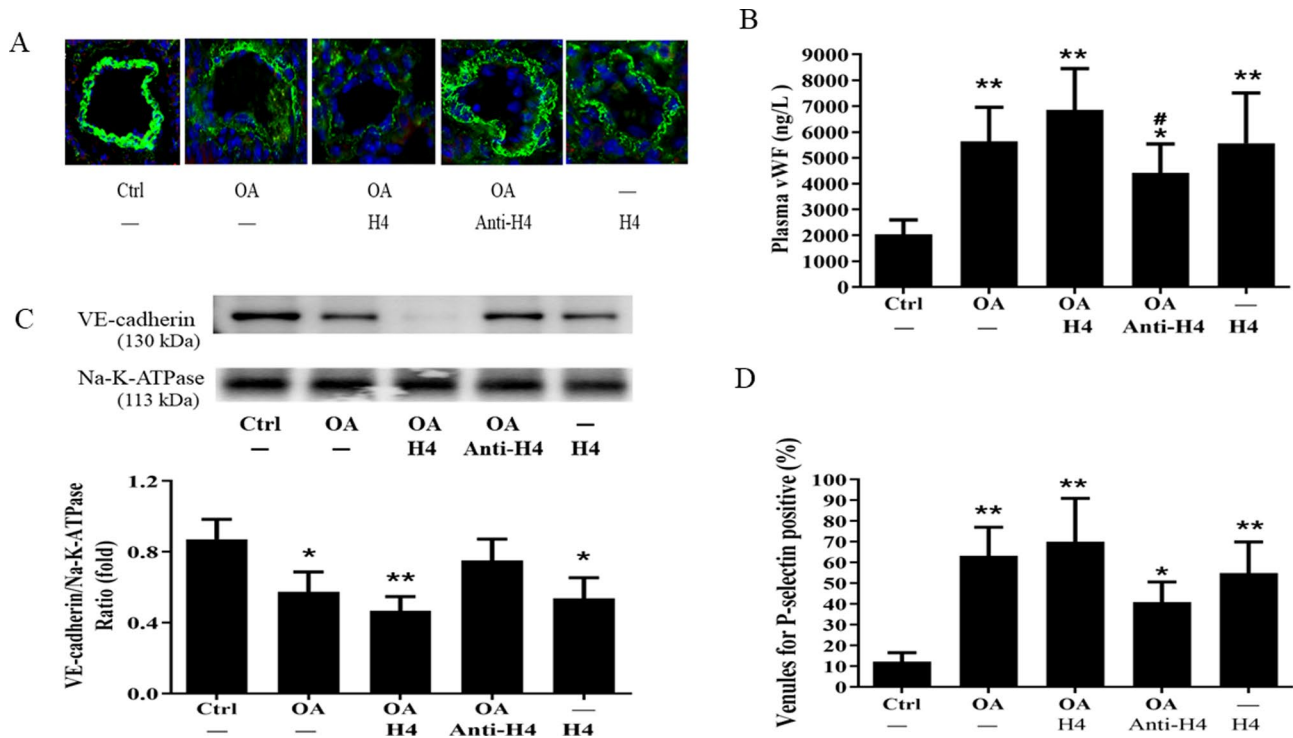


Fig. 2 Pulmonary endothelial activation in OA-induced ARDS. The changes in the pulmonary vascular glycocalyx were evaluated by immunofluorescence staining of endothelial HS (**A**) 12 h after the mice were challenged with OA (300 μ L/kg) injected intravenously. Histone H4 (10 mg/kg) or anti-H4 antibody (20 mg/kg) was injected through the tail vein 30 min prior to OA challenge. The level of circulating vWF was measured by ELISA (**B**), and the change in VE-Cadherin in the cell membrane was measured by western blot (**C**). The translocation of P-selectin in the venules was evaluated by immunohistochemical detection (**D**). Data are presented as mean \pm SD ($n=6$). The results for immunofluorescence staining and western blot are representative of three similar experiments. * $p < 0.05$, ** $p < 0.01$ compared to the control group; # $p < 0.05$, ## $p < 0.01$ compared to the OA group

caused by OA challenge, whereas the anti-H4 antibody showed an antagonizing effect on them. Impressively, histone H4 infusion alone also caused marked neutrophil infiltration and activation.

Activation effect of histone H4 on the endothelium and neutrophils in vitro

As shown in Fig. 4A and B, treatment of MLVECs with the plasma collected from OA challenged mice (OA-plasma) led to endothelial HS degradation and vWF release from WPBs compared to the control group ($p < 0.0001$). Pretreatment with histone H4 worsened HS degradation and vWF release caused by the OA-plasma, whereas the anti-H4 antibody showed an inhibitory effect to some extent. Treatment with histone H4 alone also caused evident HS degradation and vWF release. As shown in Fig. 4C, when neutrophils were treated with the OA-plasma and then exposed to MLVECs unchallenged with histone H4, the relative proportion of neutrophils adhering to MLVECs was mildly increased compared to the control group ($p = 0.1658$). On the contrary, when the treated neutrophils were exposed to MLVECs challenged with histone H4, the proportion of neutrophils adhering to the MLVECs was significantly increased ($p < 0.0001$), as shown in Fig. 4D. As shown in Fig. 4E and F, the change

in the MPO activity in the supernatant was similar to that for the neutrophil adhesion. When the neutrophils treated with the OA-plasma were exposed to unchallenged MLVECs, MPO activity was slightly increased compared to the control group ($p = 0.4886$). When the treated neutrophils were exposed to MLVECs challenged with histone H4, MPO activity was markedly increased compared to the control group ($p < 0.0001$). Pretreatment with histone H4 increased neutrophil adhesion and MPO activity further, whereas the anti-H4 antibody showed an antagonizing effect. By inhibiting the mutual binding of the endothelium and neutrophils, the blocking anti-P-selectin antibody significantly decreased the neutrophil adhesion ($p = 0.0474$) and MPO activity ($p = 0.0350$) compared to the OA-plasma group.

Roles of TLRs and calcium in histone H4 mediated endothelium activation

To study the signaling pathways involved in histone H4-mediated endothelium activation, blocking antibodies against TLR1, TLR2, TLR4, and TLR6 were used to investigate the role of TLRs. As shown in Fig. 5A and B, histone H4 treatment led to the significant degradation of membrane HS ($p < 0.0001$) and VE-Cadherin ($p = 0.0269$) in MLVECs compared to the control group,

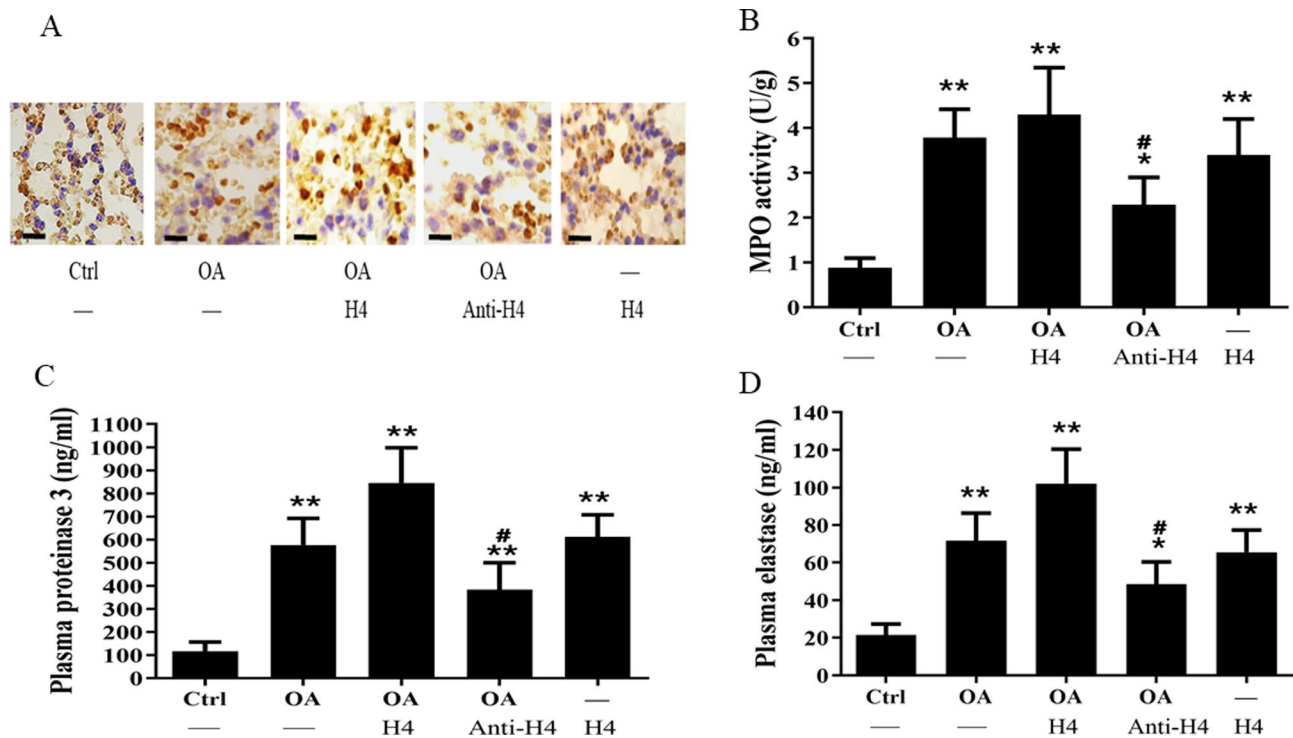


Fig. 3 Neutrophil activation in OA-induced ARDS. Neutrophil infiltration in the pulmonary tissue was examined by immunohistochemical detection of the specific marker Ly6G (A), and neutrophil activation was measured by MPO activity (B) 12 h after the mice were challenged with OA (300 μ L/kg). Histone H4 (10 mg/kg) or anti-H4 antibody (20 mg/kg) was injected intravenously 30 min prior to OA challenge. The levels of circulating proteinase 3 (C) and leukocyte elastase (D) were measured by ELISA. Data are presented as mean \pm SD ($n=6$). The immunohistochemical images are representative of three similar experiments. Scale bars: 50 μ m. * $p < 0.05$, ** $p < 0.01$ compared to the control group; # $p < 0.05$, ## $p < 0.01$ compared to the OA group

as measured by flow cytometry and western blot, respectively. Pretreatment with a blocking antibody against TLR4 distinctly inhibited the degradation of endothelial HS and VE-Cadherin. A blocking antibody against TLR2 also slightly inhibited HS and VE-Cadherin degradation. However, blocking antibodies against TLR1 and TLR6 had minimal effects. As shown in Fig. 5C and D, the release of vWF from WPBs ($p=0.0003$) and P-selectin translocation ($p < 0.0001$) in MLVECs were evident after histone H4 treatment compared to the control group. Pretreatment with the blocking antibody against TLR4 obviously reduced the release of vWF ($p=0.3655$) and P-selectin translocation ($p=0.1623$) compared to the H4-treated group. The blocking antibody against TLR2 also showed some inhibitory effect. The effects of the blocking antibodies against TLR1 and TLR6 were almost negligible. Calcium chelation with EGTA-AM was used to study the role of calcium. Calcium chelation showed little effect on endothelial HS and VE-Cadherin degradation (data not shown). However, calcium chelation evidently inhibited the release of vWF from WPBs and P-selectin translocation in a dose-dependent manner, as shown in Fig. 5E and F. Additionally, calcium chelation showed a synergistic effect with the blocking antibody against TLR4 upon the release of vWF ($p=0.0128$)

and P-selectin translocation ($p=0.0481$) compared to the H4-treated group.

Discussion

ARDS can be induced by a variety of diseases [30]. PFE is a life-threatening condition with characteristic manifestations of acute pulmonary proteinaceous edema and refractory hypoxemia [31, 32]. When nuclear histones are released passively from necrotic cells or actively by cell death such as NETosis, these extracellular histones not only exhibit bactericidal activity but also damage normal host tissues [33, 34]. The main source of histones are neutrophils which can be activated by complement C5a to form neutrophil extracellular traps (NETs) [35, 36].

In this study, histone H4 in the plasma and BALF was significantly increased after OA injection, especially when the dose of OA exceeded 300 μ L/kg. Extracellular histone H4 was closely related with the OA dose which determined the severity of acute lung injury. The pathogenic role of histone H4 was revealed further by the experimental intervention. Pretreatment with histone H4 further aggravated the pulmonary edema and death rate, while the anti-H4 antibody exerted clear protective effects.

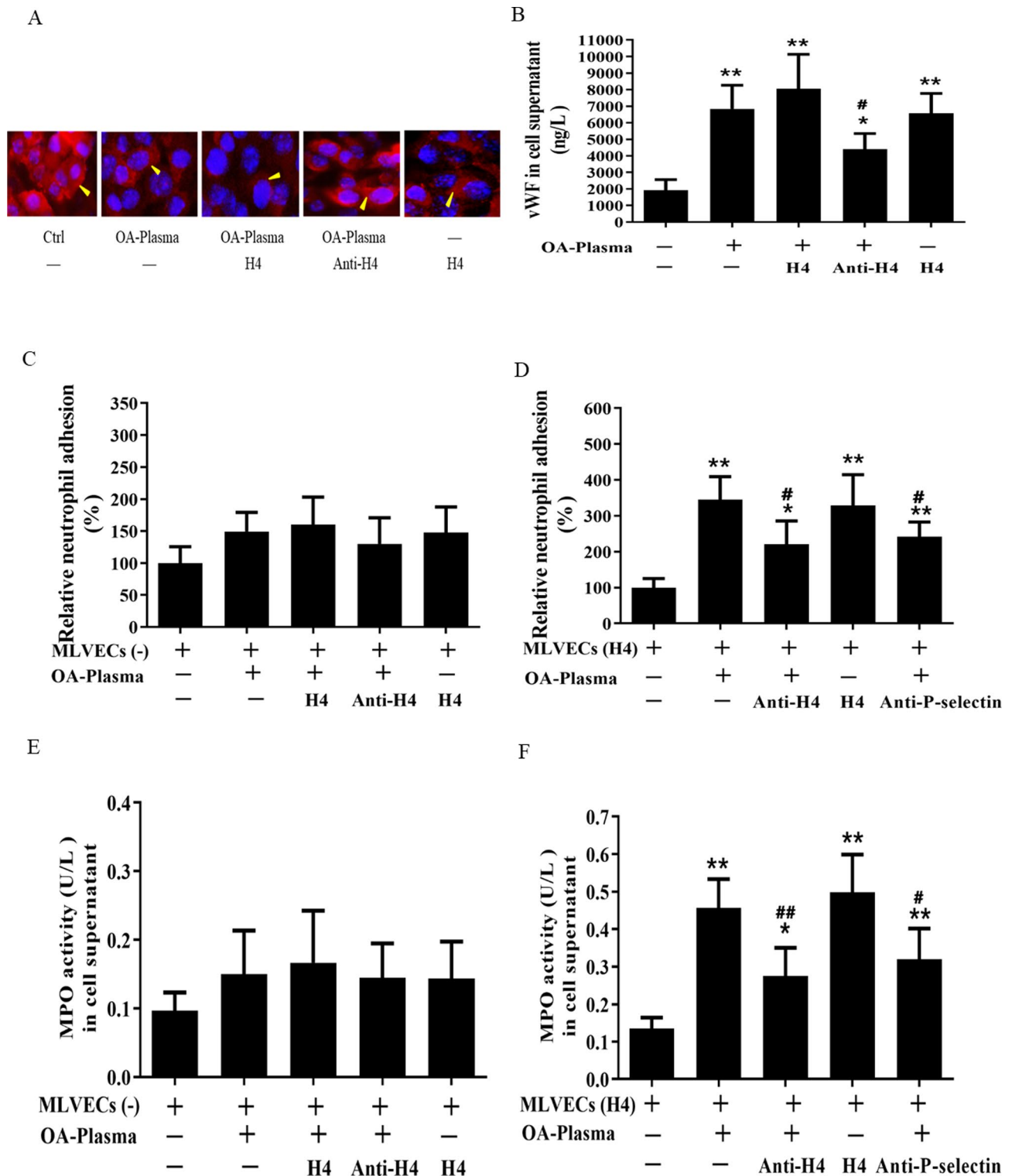


Fig. 4 Effect of histone H4 on endothelial and neutrophil activation in vitro. The changes in endothelial HS (A) and vWF in the supernatant (B) were evaluated by immunofluorescence staining and ELISA, respectively, after the MLVECs were treated with the plasma collected from OA-challenged mice (OA-plasma) for 12 h. Neutrophils were treated with the OA-plasma (12 h) and exposed to either unchallenged MLVECs or MLVECs challenged with histone H4 (15 mg/L) for six hours. The relative percentage of neutrophil adhesion to MLVECs was determined by a cell surface adhesion assay (C, D), and MPO activity in the supernatant was measured by ELISA (E, F). Histone H4 (15 mg/L), anti-H4 antibody (20 mg/L), or anti-P-selectin antibody (10 mg/L) was added to the medium one hour prior to the OA-plasma exposure. Data are presented as mean ± SD (n=6). The immunofluorescence images are representative of three similar experiments (400x). Arrowheads indicate the staining of HS. *p < 0.05, **p < 0.01 compared to the control group; #p < 0.05, ##p < 0.01 compared to the OA-plasma group

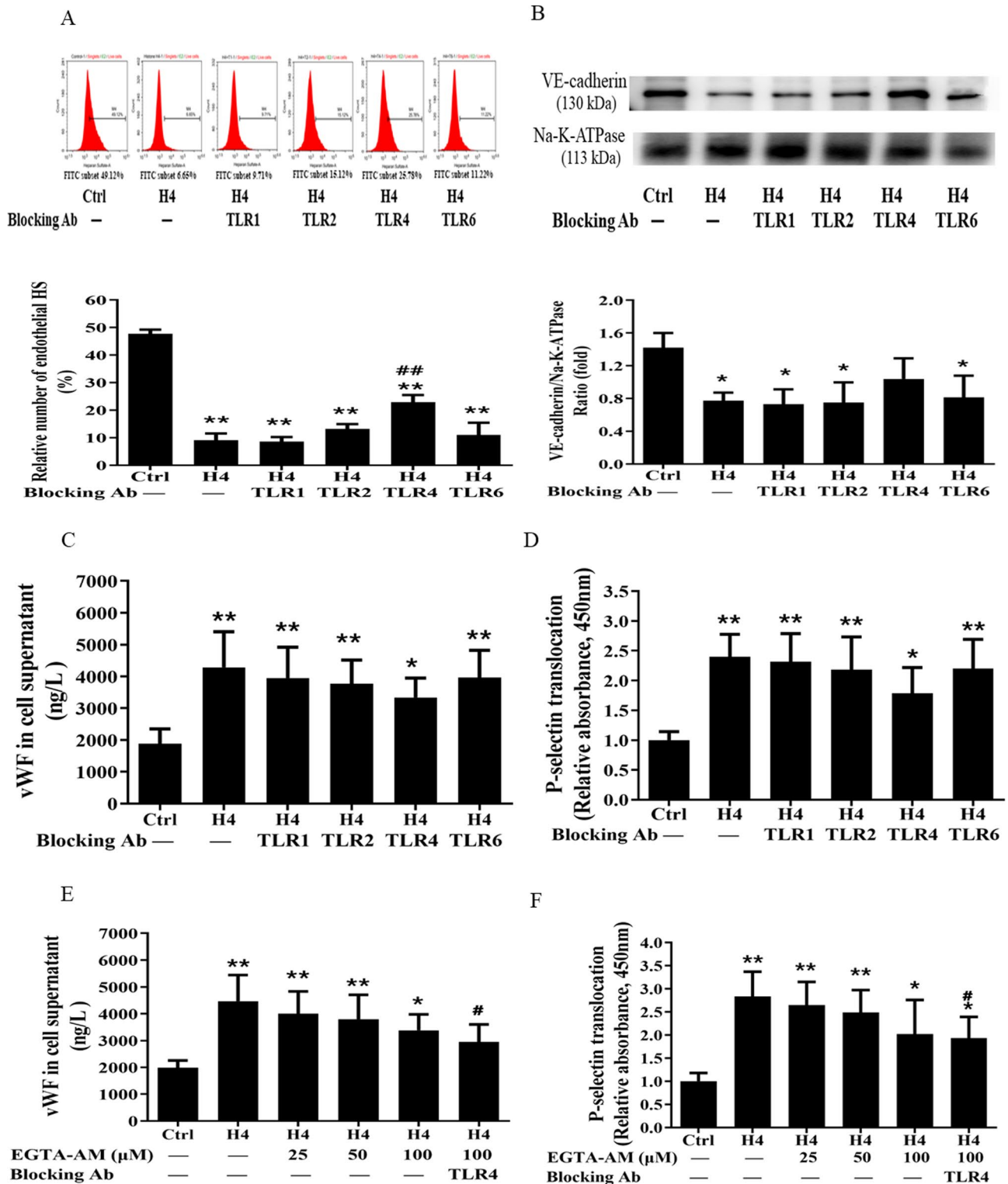


Fig. 5 TLR and calcium signaling involved in histone H4-mediated endothelium activation. After the MLVECs were challenged with histone H4 (15 mg/L) for 12 h, the changes in endothelial HS were evaluated by flow cytometry (A) while the VE-Cadherin in the cell membrane was measured by western blot (B). The vWF in the supernatant (C, E) and P-selectin translocation (D, F) were measured through ELISA. Prior to histone H4 challenge, the cells were pretreated for one hour with a blocking antibody (10 mg/L) against TLRs (TLR1, TLR2, TLR4, or TLR6) and the calcium chelator EGTA-AM (25, 50 or 100 μM). Data are presented as mean ± SD (n=6). The results for flow-cytometry and western blot are representative of three similar samples. *p < 0.05, **p < 0.01 compared to the control group; #p < 0.05, ##p < 0.01 compared to the H4 group

Endothelial and neutrophil activation is a hallmark of the ARDS pathogenesis. This study showed that significant endothelial and neutrophil activation occurred during OA-induced ARDS in mice. The endothelial activation was manifested as HS degradation, release of vWF, P-selectin translocation, and VE-Cadherin reduction. Neutrophil activation was seen through pulmonary neutrophil infiltration, elevated circulating proteinase 3 and elastase, and increased MPO activity. Pretreatment with histone H4 further worsened endothelial and neutrophil activation, but the anti-H4 antibody showed significant antagonistic effects.

The activation effect of histone H4 on endothelial cells and neutrophils was verified by *in vitro* experiments. Extracellular histone H4 could directly activate MLVECs, as measured by HS degradation and vWF release. In contrast to the activation of endothelial cells, neutrophil activation was mild when they were only challenged with exogenous histone H4, as shown by MPO activity and neutrophil adhesion assay. However, the synergistic stimulus of activated endothelia was associated with significant activation of neutrophils induced by extracellular histone H4. When the adhesion of endothelial cells with neutrophils was blocked using an anti-P-selectin antibody, the neutrophil activation was markedly inhibited. These findings suggest that neutrophil activation requires the synergistic stimulation of activated endothelium and histone H4. Furthermore, binding of neutrophils to the endothelium is a prerequisite for neutrophil activation.

Neutrophil activation begins from recruitment to lung vasculature, adhesion to pulmonary endothelium, and ends with uncontrolled activation [37, 38]. Pulmonary endothelial activation is necessary for histone H4-induced neutrophil activation. The pulmonary endothelium supplies a common platform for promoting activation of the inflammatory cascade [39, 40].

Pulmonary edema resulting from increased endothelial permeability is the keystone of ARDS. Pulmonary endothelial glycocalyx has been recognized as the main regulator of vascular structural integrity and endothelial permeability [41, 42]. As the most abundant glycosaminoglycan in pulmonary vascular endothelial glycocalyx, HS degradation mediates pulmonary endothelial hyperpermeability and consequential pulmonary edema during ARDS [43, 44]. Furthermore, multiple types of cytokines, chemokines, signaling molecules, and growth factors are reserved within HS, which are termed HS-binding proteins (HSBPs). When HS is degraded, HSBPs are released to induce the inflammatory storm [45, 46].

Weibel-Palade bodies are endothelium-specific secretory organelles that contain vWF and a variety of other inflammatory mediators, such as P-selectin, interleukin-8, and angiopoietin-2 [47]. When the endothelium detects damage, vWF is rapidly released through

exocytosis, and P-selectin is translocated to the endothelial surface for mediating endothelial activation [48]. vWF is not only a pro-thrombotic mediator but also an essential pro-inflammatory molecule. It can promote neutrophil diapedesis through the modulation of the endothelial integrity. Additionally, the released vWF can interact with the DNA of neutrophil extracellular traps to further aggravate inflammatory injury [49–51]. The P-selectin translocated to the cell surface can mediate leukocyte tethering, rolling, and diapedesis through the endothelial barrier [52–54].

VE-Cadherin is the central component of endothelial adherens junctions that regulate junctional integrity and endothelial permeability in vessels [55]. In response to an inflammatory challenge, VE-Cadherin is degraded and endocytosed through phosphorylation- and ubiquitination-dependent mechanisms. The disruption of adherens junctions is the fundamental reason for inflammation-induced acute pulmonary edema [56, 57].

TLRs are mainly distributed in the plasma membrane and include TLR1, TLR2, TLR4, TLR5, and TLR6 [58]. Our results showed that the blocking antibody against TLR4 inhibited HS degradation, P-selectin translocation, vWF release, and VE-Cadherin reduction caused by histone H4. Previous studies indicated that calcium was closely associated with extracellular histones induced injury [59, 60]. Our results showed that calcium chelation significantly inhibited the release of vWF and P-selectin translocation induced by histone H4. Furthermore, calcium chelation showed a synergistic effect with the blocking antibody against TLR4, which suggested that functional cooperation might exist between TLRs and calcium in histone H4-induced endothelial activation.

In addition to TLRs and calcium, extracellular histones may induce cell injury through other means. Extracellular histones bind directly to the phospholipids of pulmonary endothelia and cause endothelial barrier dysfunction leading to increased vascular permeability [18]. Histone H4 can mediate membrane lysis of smooth muscle cells to trigger arterial tissue damage and inflammation [61].

Damage-associated molecular patterns (DAMPs) molecules include extracellular histones, mitochondrial DNA, formyl peptides, HMBG1, etc. In addition to extracellular histones, surely other DAMPs molecules also contribute jointly to the uncontrolled inflammation in the pathogenesis of ARDS [14, 62]. Extracellular histone H4 is a cytotoxic molecule, thus it is rational that the injury effect can be inhibited through histone H4-targeted intervention. Several articles have proven that the blocking antibody or peptide targeted to histone H4 can ameliorate inflammatory damage in a few disease models such as sepsis, trauma, acute lung injury, acute pancreatitis, liver injury, and multiple organ injury [63, 64]. Both synergistic

pathogenic mechanism of the DAMPs and therapeutic potential of histone H4 need to be further studied later.

Conclusions

In conclusion, histone H4 is a pro-inflammatory and pro-thrombotic molecule in OA-induced ARDS. Histone H4 directly induces pulmonary endothelial activation. Endothelial activation is an indispensable synergistic stimulus for neutrophil activation induced by histone H4. TLRs and calcium are intimately involved in histone H4-mediated endothelium activation. The novel insights provided by this study will be helpful in clarifying the pathogenesis of ARDS caused by FES and searching for potential therapeutic application.

Supplementary Information

The online version contains supplementary material available at <https://doi.org/10.1186/s12890-024-03334-w>.

Supplementary Material 1

Acknowledgements

We thank LetPub (www.letpub.com) for its linguistic assistance during the preparation of this manuscript.

Author contributions

YLZ and SQL designed the experiment and wrote the manuscript. LG, JJT, YLZ and YRZ performed the experiments. YLZ performed the analysis studies. All authors read and approved the final manuscript.

Funding

The National Natural Science Foundation of China (Grant No. 81773374), Beijing, People's Republic of China; the Natural Science Foundation of Beijing Municipality (Grant No. 7182179), Beijing, People's Republic of China; and the Start-up Fund for Academic Leader Candidates of Peking University Third Hospital, Beijing, People's Republic of China.

Data availability

The datasets used and/or analyzed during the current study are available from the corresponding author on reasonable request.

Declarations

Ethical approval

All procedures used in this study were approved by the Peking University Animal Care and Use Committee (No. LA201783). All the experimental procedures were conducted strictly according to the U.S. NIH Guidelines for the Care and Use of Laboratory Animals.

Competing interests

The authors declare no competing interests.

Received: 22 January 2024 / Accepted: 8 October 2024

Published online: 06 January 2025

References

- Meyer NJ, Gattinoni L, Calfee CS. Acute respiratory distress syndrome. *Lancet*. 2021;398(10300):622–37.
- Beitler JR, Thompson BT, Baron RM, Bastarache JA, Denlinger LC, Esserman L, et al. Advancing precision medicine for acute respiratory distress syndrome. *Lancet Respir Med*. 2022;10(1):107–20.
- Kulkarni HS, Lee JS, Bastarache JA, Kuebler WM, Downey GP, Albaiceta GM, et al. Update on the features and measurements of experimental acute lung injury in animals: an official American thoracic society workshop report. *Am J Respir Cell Mol Biol*. 2022;66(2):e1–14.
- Ramji HF, Hafiz M, Altaq HH, Hussain ST, Chaudry F. Acute respiratory distress syndrome; a review of recent updates and a glance into the future. *Diagnosics (Basel)*. 2023;13(9):1528.
- Fujishima S. Guideline-based management of acute respiratory failure and acute respiratory distress syndrome. *J Intensive Care*. 2023;11(1):10.
- Vassiliou AG, Kotanidou A, Dimopoulou I, Orfanos SE. Endothelial damage in acute respiratory distress syndrome. *Int J Mol Sci*. 2020;21(22):8793.
- Sun X, Shikata Y, Wang L, Ohmori K, Watanabe N, Wada J, et al. Enhanced interaction between focal adhesion and adherens junction proteins: involvement in sphingosine 1-phosphate-induced endothelial barrier enhancement. *Microvasc Res*. 2009;77(3):304–13.
- van Hinsbergh VW. Endothelium—role in regulation of coagulation and inflammation. *Semin Immunopathol*. 2012;34(1):93–106.
- Nickl R, Hauser S, Pietzsch J, Richter T. Significance of pulmonary endothelial injury and the role of cyclooxygenase-2 and prostanoid signaling. *Bioeng (Basel)*. 2023;10(1):117.
- Tsai SHL, Chen CH, Tischler EH, Kurian SJ, Lin TY, Su CY, et al. Fat embolism syndrome and in-hospital mortality rates according to patient age: a large nationwide retrospective study. *Clin Epidemiol*. 2022;14:985–96.
- Lempert M, Halvachizadeh S, Ellanti P, Pfeifer R, Hax J, Jensen KO, et al. Incidence of fat embolism syndrome in femur fractures and its associated risk factors over time—a systematic review. *J Clin Med*. 2021;10(12):2733.
- Gonçalves-de-Albuquerque CF, Silva AR, Burth P, Castro-Faria MV, Castro-Faria-Neto HC. Acute respiratory distress syndrome: role of oleic acid-triggered lung injury and inflammation. *Mediators Inflamm*. 2015; 2015:260465.
- Akella A, Sharma P, Pandey R, Deshpande SB. Characterization of oleic acid-induced acute respiratory distress syndrome model in rat. *Indian J Exp Biol*. 2014;52(7):712–9.
- Murao A, Aziz M, Wang H, Brenner M, Wang P. Release mechanisms of major DAMPs. *Apoptosis*. 2021;26(3–4):152–62.
- Huang Y, Jiang W, Zhou R. DAMP sensing and sterile inflammation: intracellular, intercellular and inter-organ pathways. *Nat Rev Immunol*. 2024. <https://doi.org/10.1038/s41577-024-01027-3>.
- Xu J, Zhang X, Pelayo R, Monestier M, Ammollo CT, Semeraro F, et al. Extracellular histones are major mediators of death in sepsis. *Nat Med*. 2009;15(11):1318–21.
- Cheng Z, Abrams ST, Alhamdi Y, Toh J, Yu W, Wang G, et al. Circulating histones are major mediators of multiple organ dysfunction syndrome in acute critical illnesses. *Crit Care Med*. 2019;47(8):e677–84.
- Freeman CG, Parish CR, Knox KJ, Blackmore JL, Lobov SA, King DW, et al. The accumulation of circulating histones on heparan sulphate in the capillary glycocalyx of the lungs. *Biomaterials*. 2013;34(22):5670–6.
- Monestier M, Fasy TM, Losman MJ, Novick KE, Muller S. Structure and binding properties of monoclonal antibodies to core histones from autoimmune mice. *Mol Immunol*. 1993;30(12):1069–75.
- Tveden-Nyborg P, Bergmann TK, Jessen N, Simonsen U, Lykkesfeldt J. BCPT 2023 policy for experimental and clinical studies. *Basic Clin Pharmacol Toxicol*. 2023;111(11):13944.
- Zhang Y, Xu F, Guan L, Chen M, Zhao Y, Guo L, et al. Histone H4 induces heparan sulfate degradation by activating heparanase in chlorine gas-induced acute respiratory distress syndrome. *Respir Res*. 2022;23(1):14.
- Broccard AF, Shapiro RS, Schmitz LL, Ravenscraft SA, Marini JJ. Influence of prone position on the extent and distribution of lung injury in a high tidal volume oleic acid model of acute respiratory distress syndrome. *Crit Care Med*. 1997;25(1):16–27.
- Su X, Bai C, Hong Q, Zhu D, He L, Wu J, et al. Effect of continuous hemofiltration on hemodynamics, lung inflammation and pulmonary edema in a canine model of acute lung injury. *Intensive Care Med*. 2003;29(11):2034–42.
- Scalia R, Gefen J, Petasis NA, Serhan CN, Lefler AM. Lipoxin A4 stable analogs inhibit leukocyte rolling and adherence in the rat mesenteric microvasculature: role of P-selectin. *Proc Natl Acad Sci U S A*. 1997;94(18):9967–72.
- Zhang Y, Guan L, Yu J, Zhao Z, Mao L, Li S, et al. Pulmonary endothelial activation caused by extracellular histones contributes to neutrophil activation in acute respiratory distress syndrome. *Respir Res*. 2016;17(1):155.
- Tirupathi C, Freichel M, Vogel SM, Paria BC, Mehta D, Flockerzi V, et al. Impairment of store-operated Ca²⁺ entry in TRPC4(-/-) mice interferes with increase in lung microvascular permeability. *Circ Res*. 2002;91(1):70–6.

27. Rollin S, Lemieux C, Maliba R, Favier J, Villeneuve LR, Allen BG, et al. VEGF-mediated endothelial P-selectin translocation: role of VEGF receptors and endogenous PAF synthesis. *Blood*. 2004;103(10):3789–97.
28. Swamydas M, Lionakis MS. Isolation, purification and labeling of mouse bone marrow neutrophils for functional studies and adoptive transfer experiments. *J Vis Exp*. 2013;77:e50586.
29. Lemieux C, Maliba R, Favier J, Théorêt JF, Merhi Y, Sirois MG. Angiopoietins can directly activate endothelial cells and neutrophils to promote proinflammatory responses. *Blood*. 2005;105(4):1523–30.
30. Matthay MA, Zemans RL, Zimmerman GA, Arabi YM, Beitler JR, Mercat A, et al. Acute respiratory distress syndrome. *Nat Rev Dis Primers*. 2019;5(1):18.
31. Kao SJ, Yeh DY, Chen HI. Clinical and pathological features of fat embolism with acute respiratory distress syndrome. *Clin Sci (Lond)*. 2007;113(6):279–85.
32. Sirbu O, Sorodoc V, Floria M, Statescu C, Sascau R, Lionte C, et al. Nontrombotic pulmonary embolism: different etiology, same significant consequences. *J Pers Med*. 2023;13(2):202.
33. Kawai C, Kotani H, Miyao M, Ishida T, Jemal L, Abiru H, et al. Circulating extracellular histones are clinically relevant mediators of multiple organ injury. *Am J Pathol*. 2016;186(4):829–43.
34. Li X, Ye Y, Peng K, Zeng Z, Chen L, Zeng Y. Histones: the critical players in innate immunity. *Front Immunol*. 2022;13:1030610.
35. Grailer JJ, Ward PA. Lung inflammation and damage induced by extracellular histones. *Inflamm Cell Signal*. 2014;1(4):e131.
36. Bosmann M, Grailer JJ, Ruemmler R, Russkamp NF, Zetoune FS, Sarma JV, et al. Extracellular histones are essential effectors of C5aR- and C5L2-mediated tissue damage and inflammation in acute lung injury. *FASEB J*. 2013;27(12):5010–21.
37. Cagle LA, Linderholm AL, Franzi LM, Last JA, Simon SI, Kenyon NJ, et al. Early mechanisms of neutrophil activation and transmigration in acute lung injury. *Front Physiol*. 2022;13:1059686.
38. Reutershan J, Ley K. Bench-to-bedside review: acute respiratory distress syndrome - how neutrophils migrate into the lung. *Crit Care*. 2004;8(6):453–61.
39. Félétou M, Vanhoutte PM. Endothelial dysfunction: a multifaceted disorder (the Wiggers Award lecture). *Am J Physiol Heart Circ Physiol*. 2006;291(3):H985–1002.
40. Whitney JE, Feng R, Koterba N, Chen F, Bush J, Graham K, et al. Endothelial biomarkers are associated with indirect lung injury in sepsis-associated pediatric acute respiratory distress syndrome. *Crit Care Explor*. 2020;2(12):e0295.
41. Dull RO, Hahn RG. The glycocalyx as a permeability barrier: basic science and clinical evidence. *Crit Care*. 2022;26(1):273.
42. Jedlicka J, Becker BF, Chappell D. Endothelial glycocalyx. *Crit Care Clin*. 2020;36(2):217–32.
43. Oshima K, King SI, McMurtry SA, Schmidt EP. Endothelial heparan sulfate proteoglycans in sepsis: the role of the glycocalyx. *Semin Thromb Hemost*. 2021;47(3):274–82.
44. LaRivière WB, Schmidt EP. The pulmonary endothelial glycocalyx in ARDS: a critical role for heparan sulfate. *Curr Top Membr*. 2018;82:33–52.
45. Liao YE, Liu J, Arnold K. Heparan sulfates and heparan sulfate binding proteins in sepsis. *Front Mol Biosci*. 2023;10:1146685.
46. Li M, Pedersen LC, Xu D. Targeting heparan sulfate-protein interactions with oligosaccharides and monoclonal antibodies. *Front Mol Biosci*. 2023;10:1194293.
47. Karampini E, Fogarty H, Elliott S, Morrin H, Bergin C, O'Sullivan JM, et al. Endothelial cell activation, Weibel-Palade body secretion, and enhanced angiogenesis in severe COVID-19. *Res Pract Thromb Haemost*. 2023;7(2):100085.
48. Ochoa CD, Wu S, Stevens T. New developments in lung endothelial heterogeneity: Von Willebrand factor, P-selectin, and the Weibel-Palade body. *Semin Thromb Hemost*. 2010;36(3):301–8.
49. Ware LB, Eisner MD, Thompson BT, Parsons PE, Matthay MA. Significance of Von Willebrand factor in septic and nonseptic patients with acute lung injury. *Am J Respir Crit Care Med*. 2004;170(7):766–72.
50. Petri B, Broermann A, Li H, Khandoga AG, Zarbock A, Krombach F, et al. Von Willebrand factor promotes leukocyte extravasation. *Blood*. 2010;116(22):4712–9.
51. Luo GP, Ni B, Yang X, Wu YZ. von Willebrand factor: more than a regulator of hemostasis and thrombosis. *Acta Haematol*. 2012;128(3):158–69.
52. Lorant DE, Topham MK, Whatley RE, McEver RP, McIntyre TM, Prescott SM, et al. Inflammatory roles of P-selectin. *J Clin Invest*. 1993;92(2):559–70.
53. Takada YK, Simon SI, Takada Y. The C-type lectin domain of CD62P (P-selectin) functions as an integrin ligand. *Life Sci Alliance*. 2023;6(7):e202201747.
54. Nussbaum C, Bannenberg S, Keul P, Gräler MH, Gonçalves-de-Albuquerque CF, Korhonen H, et al. Sphingosine-1-phosphate receptor 3 promotes leukocyte rolling by mobilizing endothelial P-selectin. *Nat Commun*. 2015;6:6416.
55. Taveau JC, Dubois M, Le Bihan O, Trépout S, Almagro S, Hewat E, et al. Structure of artificial and natural VE-cadherin-based adherens junctions. *Biochem Soc Trans*. 2008;36(Pt 2):189–93.
56. Li B, Huang X, Wei J, Huang H, Liu Z, Hu J, et al. Role of moesin and its phosphorylation in VE-cadherin expression and distribution in endothelial adherens junctions. *Cell Signal*. 2022;100:110466.
57. Lampugnani MG, Dejane E, Giampietro C. Vascular endothelial (VE)-cadherin, endothelial adherens junctions, and vascular disease. *Cold Spring Harb Perspect Biol*. 2018;10(10):a029322.
58. Asami J, Shimizu T. Structural and functional understanding of the toll-like receptors. *Protein Sci*. 2021;30(4):761–72.
59. Abrams ST, Zhang N, Manson J, Liu T, Dart C, Baluwa F, et al. Circulating histones are mediators of trauma-associated lung injury. *Am J Respir Crit Care Med*. 2013;187(2):160–9.
60. Michels A, Albáñez S, Mewburn J, Nesbitt K, Gould TJ, Liaw PC, et al. Histones link inflammation and thrombosis through the induction of Weibel-Palade body exocytosis. *J Thromb Haemost*. 2016;14(11):2274–86.
61. Silvestre-Roig C, Braster Q, Wichapong K, Lee EY, Teulon JM, Berrebeh N, et al. Externalized histone H4 orchestrates chronic inflammation by inducing lytic cell death. *Nature*. 2019;569(7755):236–40.
62. Patel S. Danger-Associated molecular patterns (DAMPs): the derivatives and triggers of inflammation. *Curr Allergy Asthma Rep*. 2018;18(11):63.
63. Nicolaes GAF, Soehnlein O. Targeting extranuclear histones to alleviate acute and chronic inflammation. *Trends Pharmacol Sci*. 2024;45(7):651–62.
64. Szatmary P, Huang W, Criddle D, Tepikin A, Sutton R. Biology, role and therapeutic potential of circulating histones in acute inflammatory disorders. *J Cell Mol Med*. 2018;22(10):4617–29.

Publisher's note

Springer Nature remains neutral with regard to jurisdictional claims in published maps and institutional affiliations.